



HAL
open science

Coherence modulation and correlation of stochastic light fields

Jean-Pierre Goedgebuer, Henri Porte, Pascal Mollier

► **To cite this version:**

Jean-Pierre Goedgebuer, Henri Porte, Pascal Mollier. Coherence modulation and correlation of stochastic light fields. *Journal de Physique III*, 1993, 3 (7), pp.1413-1433. 10.1051/jp3:1993209 . jpa-00249008

HAL Id: jpa-00249008

<https://hal.science/jpa-00249008v1>

Submitted on 4 Feb 2008

HAL is a multi-disciplinary open access archive for the deposit and dissemination of scientific research documents, whether they are published or not. The documents may come from teaching and research institutions in France or abroad, or from public or private research centers.

L'archive ouverte pluridisciplinaire **HAL**, est destinée au dépôt et à la diffusion de documents scientifiques de niveau recherche, publiés ou non, émanant des établissements d'enseignement et de recherche français ou étrangers, des laboratoires publics ou privés.

Classification
Physics Abstracts
42.30 — 42.82

Coherence modulation and correlation of stochastic light fields

Jean-Pierre Goedgebuer, Henri Porte and Pascal Mollier

Laboratoire Optique P. M. Duffieux, URA CNRS 214, Faculté des Sciences, Université de Franche-Comté, 25030 Besançon Cedex, France

(Received 10 December 1992, accepted 5 April 1993)

Abstract. — We give an overview of the physical principles of coherence modulation of light that are discussed in terms of correlation of stochastic light fields such as those emitted by broadband sources. Multiplexing properties of this method are also considered in the frame of two system topologies, the series and parallel configurations, with emphasis put on source of noise inherent to coherence modulation. Applications are also reviewed in optical telecommunications, optical sensing, integrated optics and optical computing.

1. Introduction.

Coherence modulation of light is a modulation method which utilizes the coherence properties of broadband sources for encoding signals onto a light beam. One peculiarity of the method, compared to other conventional optical modulation methods, is that it allows several signals to be multiplexed on a single light beam. The physical principles make intervene correlation of stochastic light fields that are emitted by broadband sources. This paper is intended as a review of these physical principles, together with a survey of the emerging applications in the area of optical communications, optical computing and integrated optics. We place major emphasis on physical principles of coherence modulation. The paper is organized as follows. In section 2 we show how the well-known phenomenon of « fringes of superposition » can be described in terms of « side lobes of coherence » equivalent to the lateral frequency bands generated by the conventional amplitude and phase modulation techniques in the frequency domain. Section 3 deals with an extension of the previous concepts to the transmission of multiplexed signals. This allows a generalization in section 4 and a discussion on the number of transmission channels and on the dynamic range of coherence-multiplexed systems. In section 5, we show how the coherence modulation process itself induces noise in the detected signals owing to the fact that the mutual degree of coherence of « incoherent » light fields cannot be considered as negligibly small in most cases. Section 6 gives a review of most of the applications of this method which opens new trends in local fiber area network, optical sensing and also in integrated optics in which new devices suitable for coherence modulation begin to appear.

2. Fundamentals of coherence modulation.

2.1 STATISTICAL PROPERTIES OF LIGHT AND COHERENCE DEGREE. — Before specifying the principles of operation of coherence modulation of light, we turn our attention to some well-known statistical properties of the light field emitted by a broadband source, such as a white light source for instance. We assume in the following the power-spectrum of the source is Gaussian, as depicted in figure 1. The center optical frequency is f_0 and full width at half maximum is $\text{FWHM} = \Delta f$. The notations are given in figures 1a and 1b which show the power-spectrum $P(f - f_0)$ and the coherence degree $|\gamma(t')|$ of a Gaussian white light source. We also recall some properties that will be useful :

1) the light field produced by a continuous white light source is assumed to be a stationary stochastic field with an instantaneous complex amplitude $s(t)$. In the following, the notation used for the covariance function of $s(t)$ is $C(t') = \text{Re} \langle s(t) \cdot s^*(t - t') \rangle$, where s^* denotes the complex conjugate of s ;

ii) the coherence degree $|\gamma(t')|$ of the source is defined as the real part of the Fourier Transform of the power-spectrum [1] centered at $f = 0$, normalized to the power P_0 of the source :

$$|\gamma(t')| = \frac{\text{Re} \int_{-\infty}^{+\infty} P(f) \exp(j 2 \pi f t') df}{\int_{-\infty}^{+\infty} P(f) df} \tag{1}$$

with $\int_{-\infty}^{+\infty} P(f) df = P_0 = \text{power of the source.}$

After the Wiener-Khintchine theorem, the coherence degree $|\gamma|$ is related to the covariance function $C(t')$ of $s(t)$ by :

$$\text{Re} \langle s(t) \cdot s^*(t - t') \rangle = C(t') = P_0 |\gamma(t')| \cos \{2 \pi f_0 t'\} . \tag{2}$$

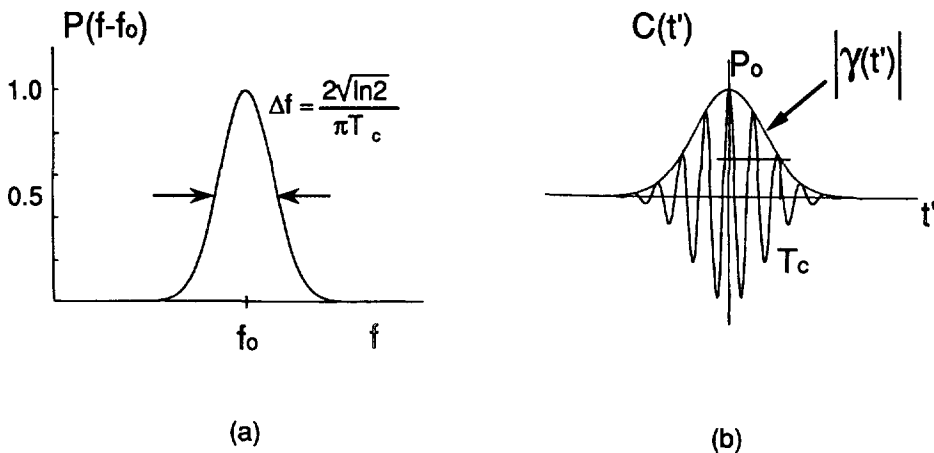


Fig. 1. — (a) Power-spectrum of a Gaussian source. (b) Covariance function of the stochastic light field emitted by the source. The envelope represents the coherence degree $|\gamma|$.

The coherence time T_c of the source is defined in the following as the halfwidth of the coherence degree at e^{-1} of its maximum ; the coherence length is $L_c = cT_c$ (c : velocity of light in vacuum).

For instance, for a source with a Gaussian power-spectrum expressed by :

$$P(f - f_0) = P_0 T_c \sqrt{\pi} \exp \left\{ - \pi^2 T_c^2 (f - f_0)^2 \right\} \tag{3}$$

we have, after equations (1) and (2) :

$$C(t') = P_0 |\gamma(t')| \cos(2\pi f_0 t') = P_0 \exp\left(-\frac{t'^2}{T_c^2}\right) \cos(2\pi f_0 t') \tag{4}$$

$$|\gamma(t')| = \exp\left(-\frac{t'^2}{T_c^2}\right) \tag{5}$$

2.2 OPTICAL CORRELATION OF STOCHASTIC LIGHT FIELDS. — Equation (2) is important since it shows that the coherence degree $|\gamma|$ can be assessed through the covariance function of the stochastic light fields emitted by a source. We recall briefly how such a covariance function can be obtained experimentally using a Michelson interferometer. In figure 2, a Michelson interferometer with an air-wedge α is illuminated in parallel light by a source whose emitted power is P_0 and power-spectrum is $P(f - f_0)$. The interferometer introduces a variable path-difference D' which corresponds to a time delay $t' = D'/c$ (c : velocity of light). At its output,

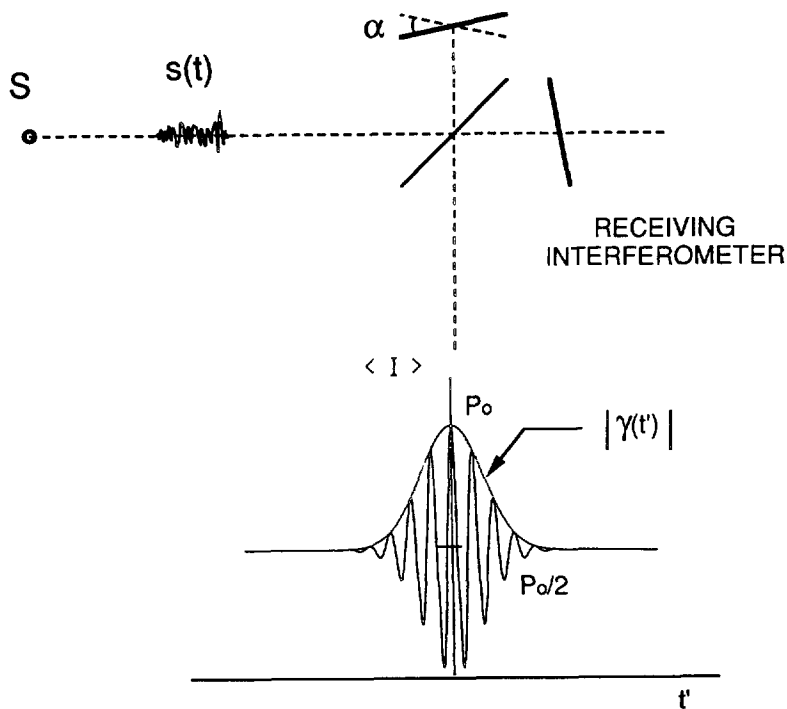


Fig. 2. — Assessing the covariance function of the light field $s(t)$ emitted by source S using a Michelson interferometer. The air-wedge α introduces a variable optical delay t' . The detected energy $\langle I \rangle$ at the output provides the covariance function of $s(t)$.

we obtain two light fields time-delayed by t' . The output light amplitude $f(t)$ is :

$$f(t) = \frac{1}{2} s(t) + \frac{1}{2} s(t - t'). \quad (6)$$

The intensity I detected at the interferometer output results from a time integration performed by the detector :

$$I = \int_0^T |f(t)|^2 dt \quad (7)$$

where T is the time integration of the detector. Assuming T is long enough to approximate integral (7) as a time average, the detected intensity is :

$$\langle I \rangle = \langle f(t) \cdot f^*(t) \rangle \quad (8)$$

where $\langle \quad \rangle$ denotes a time average.

Substituting equation (6) into (8), we obtain :

$$\begin{aligned} \langle I(t') \rangle = & \frac{1}{4} \langle |s(t)|^2 \rangle + \frac{1}{4} \langle |s(t - t')|^2 \rangle + \frac{1}{4} \langle s(t) \cdot s^*(t - t') \rangle + \\ & + \frac{1}{4} \langle s^*(t) \cdot s(t - t') \rangle = \frac{1}{2} \langle |s(t)|^2 \rangle + \frac{1}{2} \text{Re} \langle s(t) \cdot s^*(t - t') \rangle \end{aligned} \quad (9)$$

where $\langle |s(t)|^2 \rangle = P_0$.

Equation (9) indicates that the intensity $\langle I(t') \rangle$ at the output of the interferometer is the superposition of a dc term $P_0/2$ and the real part of the covariance function of the input light field. The fact that an interferometer can be described in terms of an optical correlator yielding the covariance function of the input light field is a well-known property often used in the area of ultra short light pulses.

However this point is often overlooked in conventional interferometry as continuous wave sources are of concern. For a white light source, the interference pattern observed at the interferometer output is formed by the well-known achromatic Newton's fringes. After equation (2), the latter can be regarded as the physical representation of the covariance function of the stochastic field emitted by the white light source ; the fringe envelope gives the coherence degree $|\gamma(t')|$. In the following, we show how this key property forms the basis of the so-called « coherence modulation » of light.

2.3 TOWARDS « COHERENCE MODULATION » OF LIGHT. — The basic principle of coherence modulation of light can be explained from the trivial experiment illustrated in figure 3. In figure 3a, a Mach-Zehnder interferometer is set in front of the Michelson interferometer considered in figure 2. The first interferometer is illuminated in parallel light by the cw white light source S and is adjusted on a path-difference D_1 introducing an optical delay $\tau_1 = D_1/c$ greater than the coherence time of the source. In the following, the Mach-Zehnder interferometer will be termed « coherence modulator », and the Michelson interferometer will be named « receiving interferometer ».

When propagating in the « coherence modulator » as defined above, the light field $s(t)$ emitted by the source is split into twin time-delayed light fields. The light amplitude at the output of the first interferometer is :

$$g(t) = \frac{1}{2} s(t) + \frac{1}{2} s(t - \tau_1). \quad (10)$$

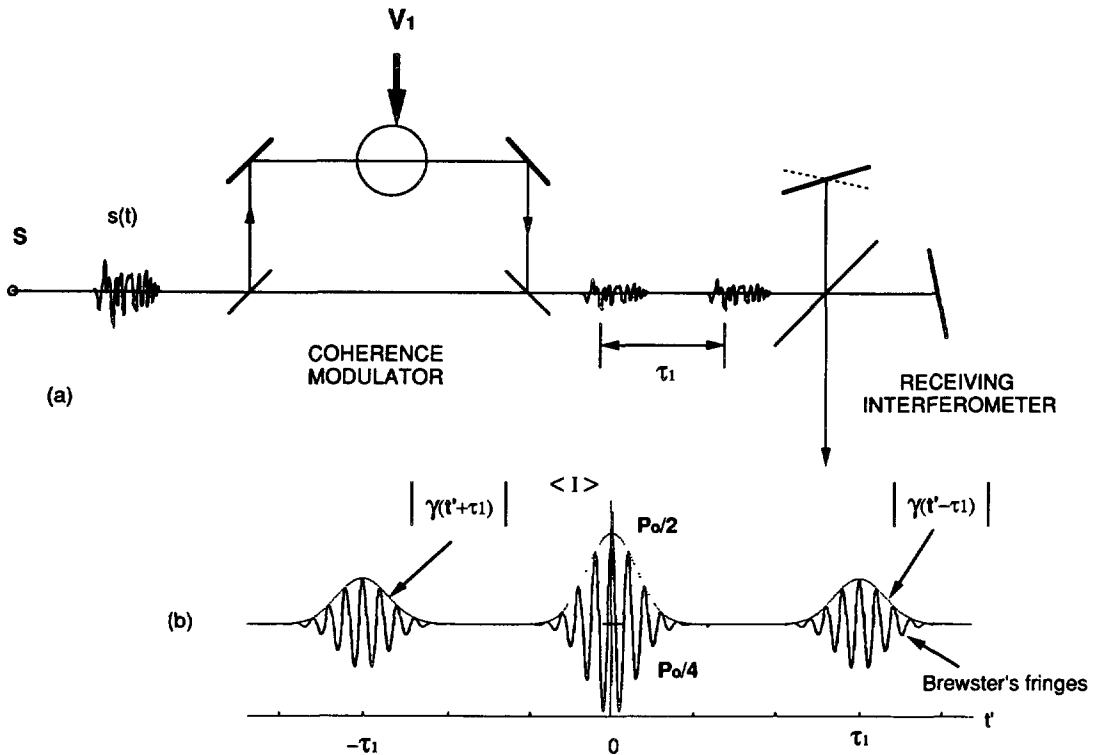


Fig. 3. — (a) Generation of Brewster's fringes using a Mach-Zehnder interferometer in tandem with a Michelson interferometer. (b) Detected power obtained at the output of the Michelson interferometer.

Note here that, in an ideal coherence modulator, no detectable interference fringe is expected since the optical delay τ_1 is greater than the coherence time. In reality a slight intensity modulation subsists due to the low mutual coherence of the twin light fields. The light field $g(t)$ serves as the input of the receiving interferometer.

At the output of the receiving interferometer, which works as an optical correlator as discussed in section 2.2, we obtain the covariance function of the light field $g(t)$. The intensity obtained at the output is given by substituting $s(t)$ by $g(t)$ in equation (9) :

$$\begin{aligned}
 \langle I(t') \rangle &= \frac{1}{2} \langle |g(t)|^2 \rangle + \frac{1}{2} \text{Re} \langle g(t) \cdot g^*(t - t') \rangle \\
 &= \frac{1}{4} \langle |s(t)|^2 \rangle + \frac{1}{4} \text{Re} \langle s(t) s^*(t - \tau_1) \rangle + \frac{1}{4} \text{Re} \langle s(t) s^*(t - t') \rangle + \\
 &\quad + \frac{1}{8} \text{Re} \langle s(t) \cdot s^*(t + \tau_1 - t') \rangle + \frac{1}{8} \text{Re} \langle s(t) \cdot s^*(t - \tau_1 - t') \rangle . \quad (11)
 \end{aligned}$$

Using equation (2), this output energy can be expressed as :

$$\langle I(t') \rangle = \frac{1}{4} P_0 + \frac{1}{4} C(\tau_1) + \frac{1}{4} C(t') + \frac{1}{8} C(t' - \tau_1) + \frac{1}{8} C(t' + \tau_1) . \quad (12)$$

The interference pattern observed at the output of the « receiving interferometer » is the superposition of a uniform background $P_0/4 + C(\tau_1)/4$ and three fringe patterns, as illustrated

in figure 3b located at $t' = 0$ and $t' = \pm \tau_1$. Each fringe pattern represents the covariance function of the white light source.

The side fringe patterns located at $t' = \pm \tau_1$ are the so-called Brewster's fringes or « fringes of superposition » [2]. Their location along t' -axis is directly related to the optical delay τ_1 of the coherence modulator. Such fringes are used for instance in white light interferometry to measure absolute distances or thicknesses of transparent samples [3]. First attempts to use such white light fringes to transmit signals have been reported by C. Delisle and P. Cielo [4].

Why « coherence modulation » of light ?

Whereas such fringes of superposition have been known for a long time, a rather new point of view consists in describing such fringes in terms of coherence modulation of light. Keeping in mind that the intensity obtained at the output of the receiving interferometer is directly related to the coherence degree of its input light, it can be seen from figures 2 and 3 that the « coherence modulator » generates two side lobes of coherence in the light issued from it (these side lobes of coherence are sketched as the envelopes of the Brewster's fringes in Fig. 3). The process may be regarded as being similar to what occurs in conventional amplitude and frequency modulations in which lateral bands are also generated, but in the temporal frequency domain. Detection of the fringes of superposition (= coherence lobes) implies the optical delays τ_1 and t' in the interferometer pair to be matched to within a fraction of the coherence time T_c of the source ; then we have $t' \approx \tau_1$ and the detected energy expressed by equation (12) becomes

$$\langle I(t') \rangle = \frac{1}{4} P_0 \left[1 + \frac{1}{8} \cos 2 \pi f_0 (t' - \tau_1) \right]. \quad (13)$$

Assume now the « coherence modulator » in figure 3 has a phase modulator driven by a voltage V_1 in one arm. Then the optical delay τ_1 can vary proportionally to V_1 . It can be clearly seen the two side patterns of fringes of superposition (and hence the two side lobes of coherence) will move along t' -axis according to the variations of τ_1 . At the output of the receiving interferometer, this results in a detectable intensity modulation which is related to the variations of τ_1 , and hence of V_1 . Assessing V_1 is achieved by determining the locations of the side lobes of coherence, i.e. of the fringes of superposition at the output of the receiving interferometer. Another possibility is to operate with a photodiode set at the inflexion point of the cos-curve (13) in order to obtain a detected energy directly proportional to V_1 . This is achieved with the interferometer pair held in quadrature in order to have a path-mismatch of $\lambda_0/4$: $t' = \tau_1 + 1/4 f_0$. When applying voltage V_1 , the optical delay of the « coherence modulator » becomes $\tau_1 + KV_1$ (K is the phase tuning rate of the phase modulator). Then the detected energy takes the form :

$$\langle I(t') \rangle = \frac{1}{4} P_0 [1 + \pi f_0 KV_1]. \quad (14)$$

This expression has been derived assuming $|\gamma(t' - \tau_1)| \approx 1$. It holds if the optical delay induced by the phase modulator is kept smaller than $\lambda_0/4$, i.e., if $V_1 < 1/4Kf_0$. In these circumstances, the system operates in the linear range of the cos-curve which corresponds to the fringes of superposition and the output energy is directly related to the signal V_1 . We will explain later how this can be achieved practically for high frequency signals used in optical communications. However the point of view discussed in this section on the basic principles of « coherence modulation » may raise several objections that will be discussed at the end of the article.

Considerations on the advantages provided by « coherence modulation » are given in next section.

3. Coherence multiplexing.

One of the main features of coherence modulation is that it allows optical signal multiplexing to be carried out — that is increasingly important in fiber telecommunication networks.

3.1 PARALLEL COHERENCE MULTIPLEXING. — Figure 4a illustrates the basic principles of a coherence modulated transmission system designed to transmit two signals simultaneously on a single transmission link such as an optical fiber for instance. The system is formed by two « coherence modulators » and the receiving interferometer (optical delay τ') described in section 2.3. Each « coherence modulator » features an optical delay τ_1 and τ_2 greater than the coherence time and is powered by a white light source $S_{1,2}$ which emits a stochastic light field $s_{1,2}(t)$. For clarity, illustration of the situation will be given taking $\tau_2 = 2 \tau_1$. First, suppose the source S_1 operates. The light field produced by the coherence modulator # 1 is

$$g_1(t) = \frac{1}{2} s_1(t) + \frac{1}{2} s_1(t - \tau_1).$$

The energy $\langle I \rangle$ at the output of the receiving interferometer is given by replacing s by s_1 in equation (11). Figure 3b shows the interference pattern thus obtained. It exhibits two side lobes of coherence which correspond to the fringes of superposition located at

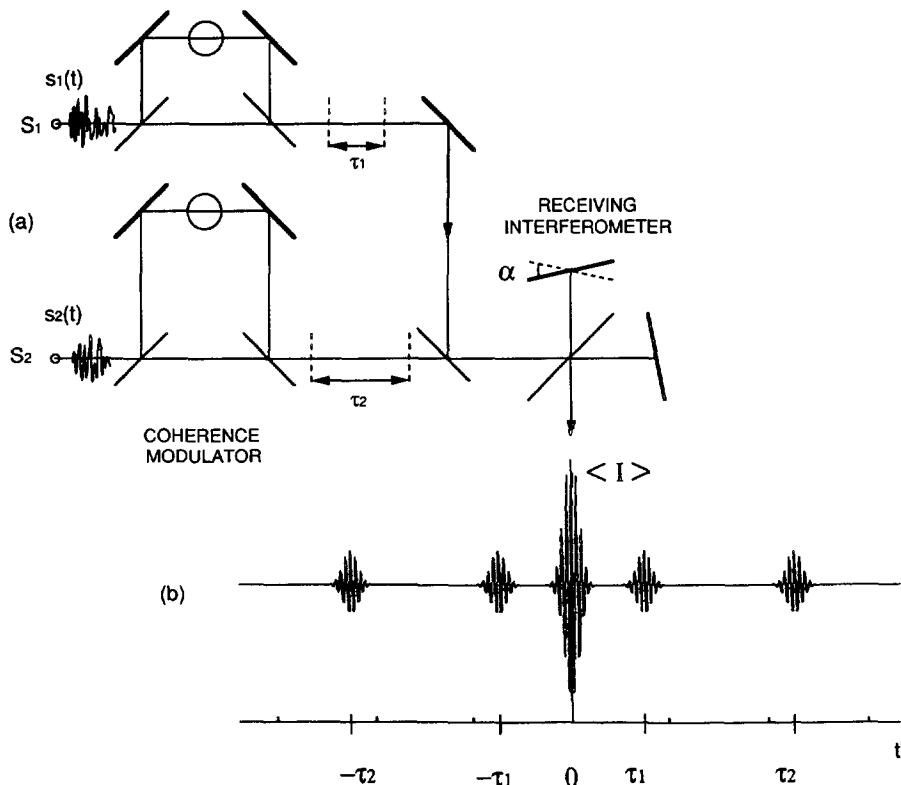


Fig. 4. — (a) Parallel topology for a coherence-multiplexed system. (b) Detected power obtained at the output of the receiving interferometers. The satellite fringes are Brewster's fringes whose localization is related to the optical delays τ_1 and τ_2 of the coherence modulators.

$t' = \pm \tau_1$. Suppose now that the source S_2 only operates. Then the light field obtained at the output of the coherence modulator # 2 is :

$$g_2(t) = \frac{1}{2} s_2(t) + \frac{1}{2} s_2(t - \tau_1).$$

The two side lobes of coherence are centered at $t' = \pm \tau_2$. Suppose now the two sources S_1 and S_2 operate in parallel. The sources being mutually incoherent, the light fields s_1 and s_2 are not correlated and we have in an ideal system $\langle s_1(t) \cdot s_2^*(t - t') \rangle = 0$. Then the power $\langle I(t') \rangle$ at the output of the receiving interferometer can be easily deduced from equation (11) :

$$\begin{aligned} \langle I(t') \rangle &= \frac{1}{4} \langle |g_1(t)|^2 \rangle + \frac{1}{4} \langle |g_2(t)|^2 \rangle + \frac{1}{4} \text{Re} \langle g_1(t) g_1^*(t - t') \rangle + \\ &+ \frac{1}{4} \text{Re} \langle g_2(t) \cdot g_2^*(t - t') \rangle = \frac{1}{8} \{P_1 + P_2 + C_1(\tau_1) + C_2(\tau_2)\} \\ &+ \frac{1}{8} C_1(t') + \frac{1}{8} C_2(t') + \frac{1}{16} C_1(t' \pm \tau_1) + \frac{1}{16} C_2(t' \pm \tau_2) \end{aligned} \quad (15)$$

with P_1, P_2 power of the sources 1 and 2.

The interference pattern thus obtained is formed by the incoherent superposition of the previous interference patterns as shown in figure 4b. We obtain now four side lobes of coherence centered at $t' = \pm \tau_1$ and $t' = \pm \tau_2$ respectively. Then, transmission and detection of two electric signals V_1 and V_2 is carried out by determining the locations of the fringes of superposition obtained at the receiving interferometer. This can be extended to a number of N signals by using an array of N parallel coherence modulators powered by N sources. This multiplexing scheme offers the greatest potential in optical telecommunications and sensor arrays with the possibility of using sources with no stringent requirements on the source linewidth and on the center frequency of laser emission, in contrast to wavelength multiplexing and demultiplexing methods.

3.2 SERIES COHERENCE MULTIPLEXING. — Figure 5a shows another coherence multiplexing scheme in which the « coherence modulators » are now set in cascade. For simplicity, we limit the discussion to only two « coherence modulators » but it can be extended to a cascade with a higher number of modulators. Each coherence modulator features an optical delay τ_1 and τ_2 greater than the coherence time. For clarity, the situation is illustrated taking $\tau_2 = 3 \tau_1$. The situation is completely different from the previous case in so far as the light emitted by the first coherence modulator is used as the input of the second one. Then, the light fields can be written as :

* output of coherence modulator # 1 :

$$g_1(t) = \frac{1}{2} s(t) + \frac{1}{2} s(t - \tau_1) \quad (16)$$

* output of coherence modulator # 2 :

$$g_2(t) = \frac{1}{2} g_1(t) + \frac{1}{2} g_1(t - \tau_2). \quad (17)$$

This light field serves as the input of the receiving interferometer.

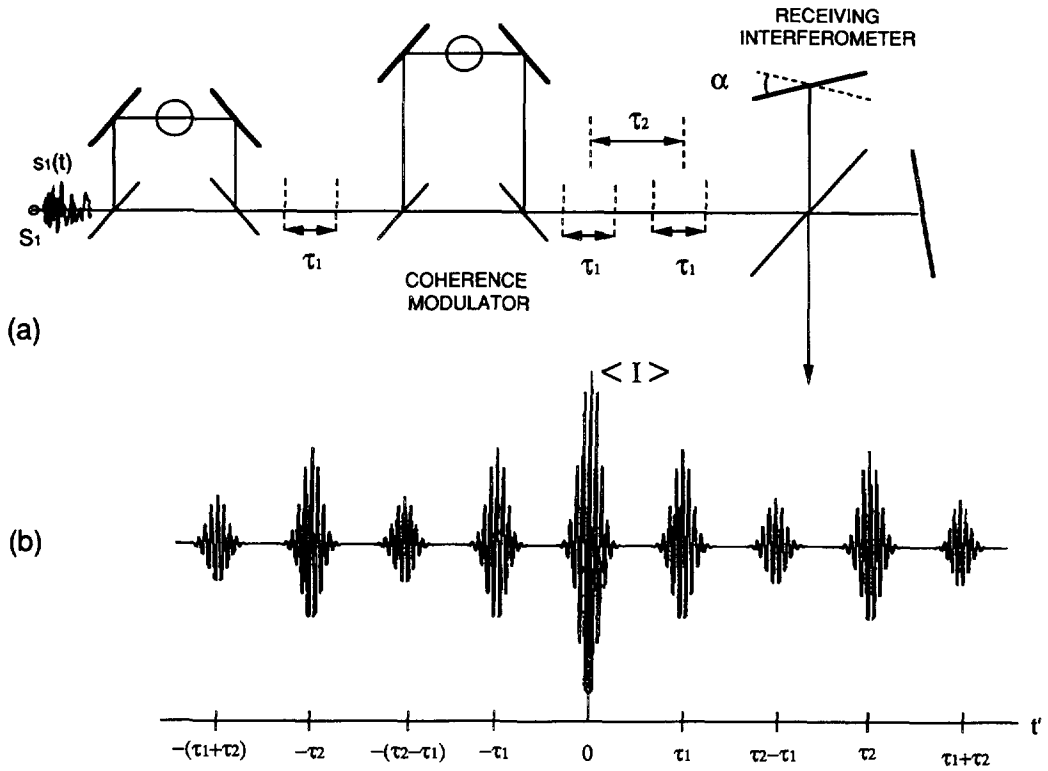


Fig. 5. — (a) Series topology for a coherence-multiplexed system. (b) Detected power at the output of the receiving interferometer. Signal Brewster's fringes ($\pm \tau_1, \pm \tau_2$) are obtained together with cross-term Brewster's fringes ($\pm \tau_1 \pm \tau_2$).

Thus, after equation (11), the power $\langle I(t') \rangle$ at the output of the receiving interferometer is related to the covariance function of $g_2(t)$ by :

$$\langle I(t') \rangle = \frac{1}{2} \langle |g_2(t)|^2 \rangle + \frac{1}{2} \text{Re} \langle g_2(t) \cdot g_2^*(t - t') \rangle . \tag{18}$$

Finally, we obtain :

$$\begin{aligned} \langle I(t') \rangle = & \left[\frac{1}{8} P_0 + \frac{1}{8} C(\tau_1) + \frac{1}{8} C(\tau_2) + \frac{1}{16} C(\tau_1 + \tau_2) + \frac{1}{16} C(\tau_2 - \tau_1) \right] + \\ & + \left[\frac{1}{8} C(t') + \frac{1}{16} C(t' \pm \tau_1) + \frac{1}{16} C(t' \pm \tau_2) \right. \\ & \left. + \frac{1}{32} C\{t' \pm (\tau_2 - \tau_1)\} + \frac{1}{32} C\{t' \pm (\tau_1 + \tau_2)\} \right] . \tag{19} \end{aligned}$$

Figure 5b shows the interference pattern thus obtained. The terms in the first brackets represent a dc term. The covariance function C decaying with optical delay, the value of the dc term can be approximated to $P_0/8$. The terms in the second brackets represent nine packets of fringes of superposition located at $t' = 0, \pm \tau_1, \pm \tau_2, \pm (\tau_2 - \tau_1)$ and $\pm (\tau_1 + \tau_2)$. Obviously, signal demultiplexing is carried out using the fringes located at $t' = \pm \tau_1$ and $t' = \pm \tau_2$. The other fringes which are located at $\pm \tau_2 \pm \tau_1$ correspond to cross-terms which may cause crosstalk as will be discussed in paragraph 5.2.

The situation becomes very complex when increasing the number of coherence modulators. The values of the optical delays $\tau_1, \tau_2, \dots, \tau_N$ must be chosen very carefully, as will be discussed in section 5.3. At the output of the receiving interferometer, the interference pattern thus obtained is formed by packets of fringes located at $t' = \tau_1, \tau_2, \dots, \tau_N$ and also at all combinations such as $t' = \pm \tau_i \pm \tau_j, t' = \pm \tau_i \pm \tau_j \pm \tau_k, \dots$. The fringes of interest for signal demultiplexing are those located at $t' = \tau_1, \tau_2, \dots, \tau_N$. A practical implementation of such an array of coherence modulators will be illustrated in the area of optical communications in section 6.

4. Generalization to N coherence-multiplexed signals.

In previous sections, the discussion was limited to systems with only two channels for simplicity's sake in order to point out the physical background. However in an effective transmission system, one may wonder what is the evolution of the detected signals, especially in terms of dynamic range and modulation depth, as the number of channels increases.

4.1 PARALLEL CONFIGURATIONS WITH N CHANNELS. — Consider $N \ll$ « coherence modulators » with optical delays $\tau_1, \tau_2, \dots, \tau_N$, powered in parallel by N sources. We assume that light produced by such modulators is launched in a receiving interferometer via a $N \times 1$ coupler (N inputs, 1 output). The optical delay of the receiving interferometer is t' . The light field at the output of the i -th modulator is, after equation (13) :

$$g_i(t) = \frac{1}{2} s_i(t) + \frac{1}{2} s_i(t - \tau_i) \quad (20)$$

where $s_i(t)$ is the light field emitted by source S_i . The resulting light field $g(t)$ at the entrance of the receiving interferometer is :

$$g(t) = \frac{1}{\sqrt{N}} \cdot \sum_{i=1}^N g_i(t). \quad (21)$$

The term $1/\sqrt{N}$ appears because of the unavoidable losses which occur when light fields from N sources are combined by a $N \times 1$ coupler. Then, for an ideal system powered by mutually incoherent sources, the power detected at the output of the receiving interferometer is, after equation (15) :

$$\begin{aligned} \langle I(t') \rangle &= \frac{1}{2} |g(t)|^2 + \frac{1}{2} \text{Re} \langle g(t) g^*(t - t') \rangle \\ &= \frac{1}{4N} \left[\sum_{i=1}^N \left\{ P_i + C_i(\tau_i) + C_i(t') + \frac{1}{2} C_i(t' \pm \tau_i) \right\} \right]. \end{aligned} \quad (22)$$

The two first terms correspond to a dc term whose value can be approximated to $\sum P_i/4N$. The last terms correspond to $2N$ patterns of fringes of superposition centered at $t' = \pm \tau_1, \pm \tau_2, \dots, \pm \tau_N$. The fringe frequency in each pattern is related to the center frequency of the corresponding source. As an illustration, the interference pattern thus obtained is sketched in figure 6 for $N = 4$ channels which have optical delays ruled by the arithmetic series 1, 2, 3, 4. As the receiving interferometer is closely matched to the i -th channel ($t' \approx \tau_i$), and assuming the sources have the same power P_0 , the detected power takes the form :

$$\langle I(t') \rangle = \frac{P_0}{4} \left[1 + \frac{1}{2N} \cos \{ 2 \pi f_0(t' - \tau_i) \} \right]. \quad (23)$$

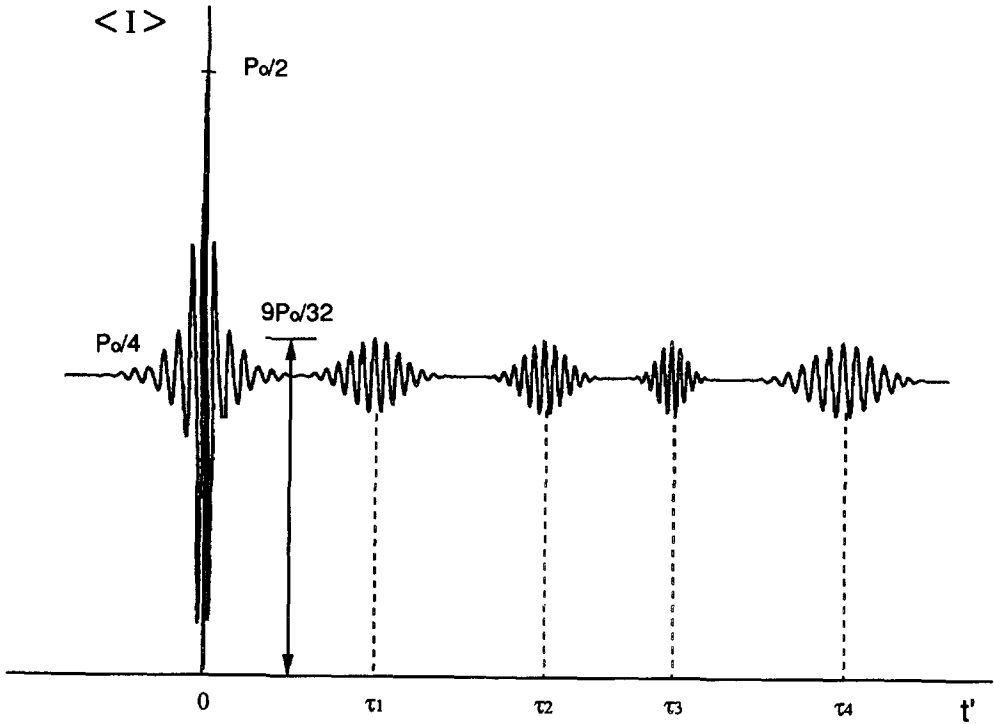


Fig. 6. — Detected power obtained at the output of the receiving interferometer vs. its optical delay, for a four-channel parallel system designed with carriers $\tau_1, 2 \tau_1, 3 \tau_1, 4 \tau_1$.

This expression has been derived by setting $|\gamma'(t' - \tau_i)| = 1$ and $C_i(\tau_i), C_i(t'), C_i(t' + \tau_i) = 0$ for an ideal system with no crosstalk (this latter point is justified in Sect. 5). Expression (23) shows that the modulation depth is $1/2 N$ and, hence, decreases with increasing the number of channels. This poses a limit to the maximum number of channels in parallel topologies.

4.2 SERIES CONFIGURATIONS WITH N CHANNELS. — Consider an array of coherence-multiplexed emitters formed by N cascaded « coherence modulators » with optical delays $\tau_1, \tau_2, \dots, \tau_N$, in tandem with a receiving interferometer with an optical delay t' . The system is powered by a single source with power P_0 . The light at the output of the series of the N modulators can be expressed *via* a series of convolution products :

$$g(t) = s(t) \otimes \frac{1}{2} \{ \delta(t) + \delta(t - \tau_1) \} \otimes \frac{1}{2} \{ \delta(t) + \delta(t - \tau_2) \} \otimes \dots \otimes \frac{1}{2} \{ \delta(t) + \delta(t - \tau_N) \} = \frac{1}{2^N} s(t) \otimes \prod_{i=1}^N \{ \delta(t) + \delta(t - \tau_i) \} \quad (24)$$

where $s(t)$ is the initial light field emitted by the source. \otimes stands for a convolution products and \prod for a series of convolution products. The light field $g(t)$ serves as the input of the

receiving interferometer. Then the power detected at its output is, after equation (18) :

$$\begin{aligned} \langle I(t') \rangle &= \frac{1}{2} |g(t)|^2 + \frac{1}{2} \text{Re} \langle g(t) g^*(t-t') \rangle \\ &= \frac{1}{2^{2N+1}} \left[2^N P_0 + \text{Re} \langle s(t) s^*(t-t') \rangle \otimes \prod_{i=1}^N \{ 2 \delta(t') + \delta(t' \pm \tau_i) \} \right]. \end{aligned} \quad (25)$$

The interference pattern described by expression (25) is formed by a uniform background $P_0/2^{2N+1}$ with patterns of fringes of superposition corresponding to the second term. A full analysis of this latter term [5] shows that it corresponds to 3^N groups of fringes of superposition located at $t' = 0, \pm \tau_1, \pm \tau_2, \dots, \pm \tau_N$ and at all combinations such as $t' = \pm (\tau_i \pm \tau_j \pm \tau_k), t' = \pm (\tau_i \pm \tau_j \pm \dots \pm \tau_N)$, etc. The signal fringes used for the demultiplexing process are those located at $t' = \pm \tau_1, \dots, \pm \tau_N$ while the others are cross-term fringes. Sakai and Parry [6] have proposed a more compact form to express the optical delays corresponding to these cross-term fringes :

$$t' = \sum_{i=1}^N \varepsilon_i \tau_i \quad (26)$$

where $\varepsilon_i \in \{-1, 0, 1\}$ and $\sum_{i=1}^N \varepsilon_i^2 \neq 1$.

The optical delays τ_i in the modulators must be chosen such that none of them is a member of the set defined in (26). This point is discussed in paragraph 5.3. As an illustration, figure 7 shows the interference pattern obtained for a three channel system with optical delays $\tau_1, \tau_2 = 3 \tau_1$ and $\tau_3 = 8 \tau_1$.

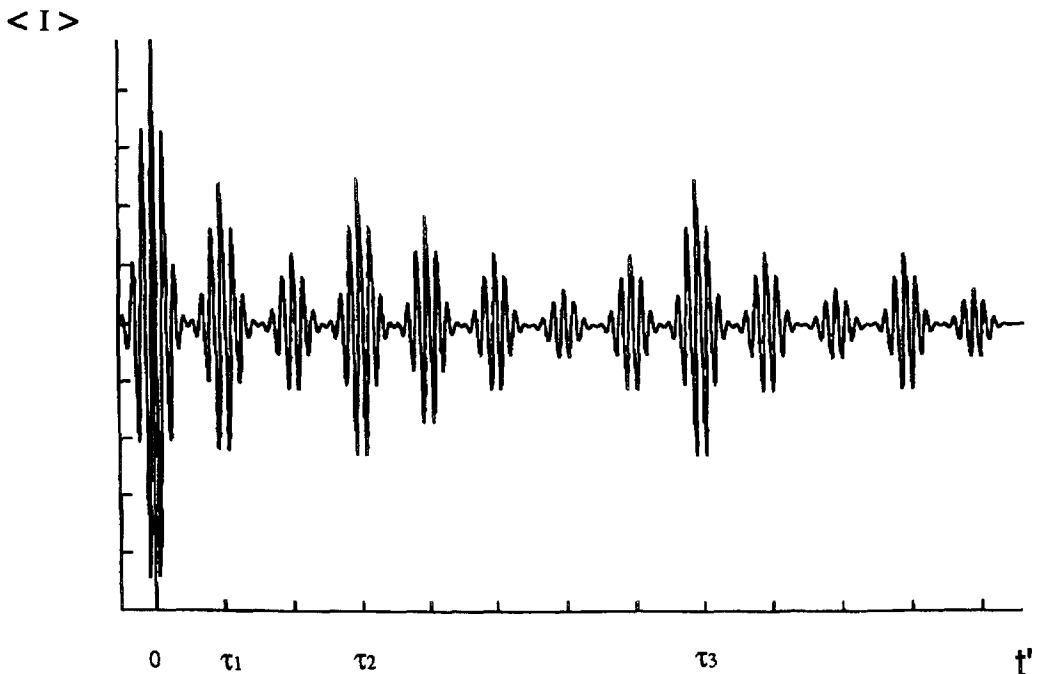


Fig. 7. — Detected power obtained at the output of the receiving interferometer vs its optical delay, for a three-channel series system designed with carriers $\tau_1, 3 \tau_1, 8 \tau_1$.

Assume now the receiving interferometer is closely matched to the i -th coherence modulator : $t' \approx \tau_i$. Then the detected power reduces to :

$$\langle I(t') \rangle = \frac{P_0}{2^{N+1}} \left[1 + \frac{1}{2} \cos \{2 \pi f_0(t' - \tau_i)\} \right]. \quad (27)$$

Expression (27) is the response of the receiving interferometer for an ideal system with no crosstalk. It shows that the modulation depth is 50 % and, hence, is independent of the number N of channels whereas the modulation depth decreases proportionally to $1/2 N$ with increasing N in the parallel topology. The series scheme is more advantageous from that point of view. However note that the signal power is $1/2^{N+2}$ and, hence, decreases more rapidly with increasing the number of channels than in the parallel configuration in which the signal power is $1/8 N$. Practically it means that a series configuration requires photodetectors with very low sensitivity while a parallel configuration requires photodetectors exhibiting a wide dynamic range.

5. Noise in coherence-modulated systems.

In this section, we limit the discussion to noise generated by the physical process attached to coherence modulation itself. We do not consider electrical or phase noise associated to photodetectors or environmental conditions.

5.1 PHASE-INDUCED INTENSITY NOISE. — When interferometers with gross path mismatch greater than the coherence length are used, the « incoherent » light fields which mix from the various optical paths still interfere due to their mutual coherence which cannot be considered as negligibly small. It results in an intensity noise which is generated physically by the random fluctuations of the phase of the initial light field emitted by the source. This noise is termed « phase-induced intensity noise ». It can be ascertained by returning to the single coherence-modulated interferometer pair shown in figure 3 and by assuming the two interferometers have their optical delays matched one to each other within a fraction of the coherence time : $t' \approx \tau_1$. Then the detected signal at the system output is given by, after equations (12) and (4) :

$$\begin{aligned} \langle I(t') \rangle = \frac{P_0}{8} \{ & 2 + |\gamma(t' - \tau_1)| \cos [2 \pi f_0(t' - \tau_1)] + 2 |\gamma(\tau_1)| \cos [2 \pi f_0 \tau_1] + \\ & + 2 |\gamma(t')| \cos [2 \pi f_0 t'] + |\gamma(t' + \tau_1)| \cos [2 \pi f_0(t' + \tau_1)] \} \quad (28) \end{aligned}$$

and finally we have, taking $|\gamma(t' - \tau_1)| = 1$ and neglecting the three last terms :

$$\langle I(t') \rangle = \frac{P_0}{8} \{ 2 + \cos [2 \pi f_0(t' - \tau_1)] \}. \quad (29)$$

In reality, in taking the mean power $\langle I \rangle$ as the expected value of the detected signal, we have assumed the detector has an infinite time of integration and, hence, we have averaged out the signal intensity noise $I - \langle I \rangle$ which is present in practice. The latter can be ascertained from calculations reported by Kersey and Dandridge [7]. Figure 8 shows the results for a single unbalanced Mach-Zehnder interferometer powered by laser diodes with various coherence lengths. The noise level peaks when the optical path difference equals the coherence length L_c , and decreases beyond L_c .

Coming back to our interferometer pair, it can be clearly seen now why the three last terms in equation (28), which denote the contributions of $|\gamma(\tau_1)|$ and $|\gamma(2 \tau_1)|$, are principally

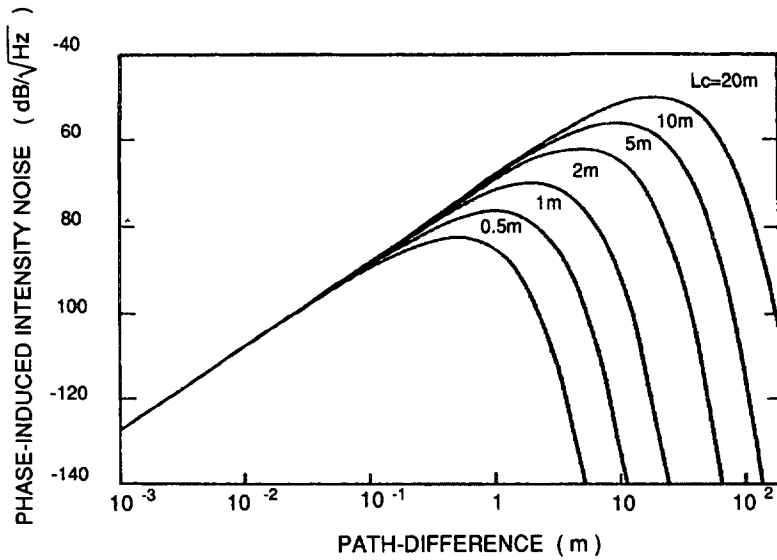


Fig. 8. — Phase-induced intensity noise obtained with an unbalanced Mach-Zehnder interferometer, for different values of the coherence length (after Kersey and Dandridge [7]).

responsible for the generation of this excess noise. Hence, low noise levels imply the use of large optical delays and short coherence lengths.

The statistical nature of this noise depends on the number of interferometers and on the system topology, as well as on the nature of the initial phase noise of the source. The latter can be modeled as a Wiener-Levy stochastic process for a single mode laser diode, or as a Gaussian random process for a thermal source. Considerations on the spectral power density of this noise are reported by Brooks *et al.* [8], and Wentworth [9] for singlemode laser diodes, thermal sources, superluminescent diodes and multimode laser diodes.

5.2 INTERMODULATION NOISE. — This type of noise appears when several signals are coherence-multiplexed. This results in crosstalk between the signals. In parallel configurations, this can be evaluated from figure 4, in which two « coherence modulators » are used in parallel to perform coherence multiplexing. Assume the receiving interferometer is matched to coherence modulator # 2 within a fraction of the coherence time : $t' \approx \tau_2$. Under these conditions, the detected output power is, after equation (15) :

$$\begin{aligned}
 \langle I(t') \rangle = & \frac{1}{8} P_1 + \frac{1}{8} P_2 + \frac{1}{16} P_2 |\gamma_2(t' \pm \tau_2)| \cos [2 \pi f_2(t' \pm \tau_2)] + \\
 & + \frac{1}{16} P_1 |\gamma_1(\tau_1)| \cos [2 \pi f_1 \tau_1] + \frac{1}{16} P_1 |\gamma_1(t' \pm \tau_1)| \cos [2 \pi f_1(t' \pm \tau_1)] \\
 & + \frac{1}{8} P_1 |\gamma_1(t')| \cos [2 \pi f_1 t'] + \frac{1}{8} P_2 |\gamma_2(t')| \cos [2 \pi f_2 t'] \\
 & + \frac{1}{16} P_2 |\gamma_2(\tau_2)| \cos [2 \pi f_2 \tau_2].
 \end{aligned} \tag{30}$$

In the ideal case, $|\gamma_{1,2}(\tau_{1,2})|, |\gamma_{1,2}(t' + \tau_{1,2})| = 0$ and $|\gamma_2(t' - \tau_2)| = 1$. Then, the output power has the form :

$$\langle I(t') \rangle = \frac{1}{8} P_1 + \frac{1}{8} P_2 + \frac{1}{16} P_2 \cos \{2 \pi f_2(t' - \tau_2)\}. \tag{31}$$

This expression represents the idealized response of the receiving interferometer matched to coherence modulator # 2. In reality, however, crosstalk results owing to the interferometric conversion of the phase delay τ_1 produced by coherence modulator # 1. The third term in equation (30), which denotes the contribution from $|\gamma_1(\tau_1)|$ attached to modulator # 1, is responsible for the generation of this crosstalk.

The maximum amplitude of this crosstalk is $|\gamma_1(\tau_1)|$. A second source of crosstalk comes from the fifth term *via* $|\gamma_1(t' - \tau_1)|$. Hence, crosstalk can be decreased to any desired level by using large values of τ_1 and of $t' - \tau_1$ (or of $\tau_2 - \tau_1$ since $t' = \tau_2$ in the example used). Another important conclusion is that crosstalk level is closely related to the profile of the coherence degree of the source, and, hence, to the profile of its spectral line. As an illustration, figure 9 shows the evolution of crosstalk for a parallel coherence-multiplexed system formed by two coherence modulators with optical delays $\tau_1, \tau_2 = 2 \tau_1$, powered by sources exhibiting identical coherence lengths but with Gaussian, Lorentzian and \cos^2 spectra. This shows clearly that crosstalk decreases with increasing τ_1 , and may vary by several orders of magnitude according to the type of sources used.

The situation is very similar in series systems. Referring to figure 5b, it can be seen that when the receiving interferometer is matched to coherence modulator # 2 ($t' = \tau_2$) for instance, the detected power is corrupted by intermodulation noise generated principally by the satellite lobes of coherence centered at $t' = \tau_1 + \tau_2$ and $t' = \tau_2 - \tau_1$. These satellite lobes of coherence, which feature a Gaussian profile in the model used, are responsible for the generation of crosstalk. Here also, crosstalk is closely related to the values of the optical delays

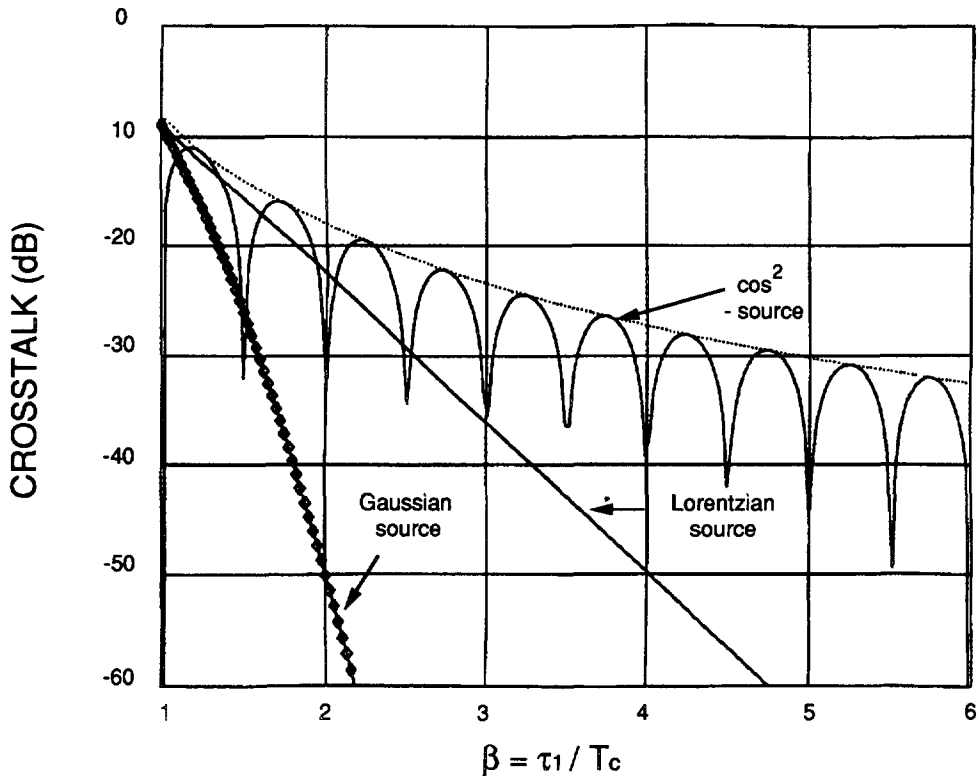


Fig. 9. — Intermodulation noise in a coherence-multiplexed system for different lineshapes.

τ_1, τ_2 set in cascade, and also to the profile of the power-spectrum of the source. A complete discussion can be found in reference [10], in which it is shown that crosstalk down to -30 dB can be easily achieved in practical systems. This opens up straightforward applications in the area of optical communications in which stringent conditions on crosstalk are generally required.

5.3 PERMISSIBLE OPTICAL DELAYS. — The sequence of optical delays is another key point of coherence multiplexing since it determines the phase-induced intensity noise and intermodulation noise. As mentioned above, no overlap should occur between the satellite lobes of coherence in order to prevent channel crosstalk. Hence, the choice of the permissible optical delays introduced in the « coherence modulators » is of major importance. Another issue relevant to the design of a coherence multiplexed system is the compactness of the system, i.e., the maximum possible value of the optical delay.

This maximum value depends on the nature of the interferometers : polarimetric interferometers featuring optical delays greater than some centimeters seem non practicable, while optical delays up to several meters can be implemented using fiber Mach-Zehnder interferometers. Compact sequences of optical delays are required especially for systems with a high number of modulators. The nature of the system determines the sequence of optical delays, as discussed hereafter.

Parallel architectures. — If the crosstalk level has to be identical in each channel, the lobes of coherence corresponding to each of the channels as shown in figure 4 have to be equidistant. Obviously, this means that the sequence of permissible optical delays for a system with N channels must be ruled by the arithmetic series of numbers $m_i = 1, 2, 3, \dots, N$. If τ_1 is the starting value of the first optical delay, the permissible optical delays are :

$$\tau_1, 2 \tau_1, 3 \tau_1, \dots, N \tau_1. \quad (32)$$

The starting value τ_1 is determined according to the level of crosstalk tolerable in each of the channels. It can be deduced from figure 9. For instance, for Gaussian sources, a crosstalk of -25 dB is obtained when the ratio between τ_1 and the coherence time T_c is $\beta = \tau_1/T_c = 1.5$. For a source with a coherence length $L_c = cT_c = 30$ micrometers (e.g. a superluminescent diode), this implies the path-difference $D_1 = c\tau_1$ of the first « coherence modulator » to be 45 micrometers, then the other permissible path-differences expressed in micrometers are 90, 135, 180, 225, .

Series architectures. — Analysis of the permissible optical delays which lead to a tolerable amount of crosstalk in each channel of series topologies is much more complex than in parallel configurations. The output signal of the receiving interferometer contains a number of spurious intermodulation terms attached principally to the cross-term fringes of superposition defined in paragraph 3.2. The optical delay τ_i of the i -th interferometer in the array must be chosen so that there is no overlap between these cross-term signals and the desired signal from this interferometer. A detailed analysis of the permissible optical delays is given by Blotekjaer *et al.* [11]. It is shown that the suitable optical delays τ_i ($i = 1, 2, \dots, N$) must be chosen such that none of them is a member of the set of time delays defined in equation (26) which correspond to the cross-term lobes of coherence. This problem of choosing these permissible optical delays does not have a unique solution. The solutions all exhibit exponential growth which severely limits the number of transmitters which may be arrayed in series. We give hereafter two of the possible recursive expressions for possible choices of series of numbers m_i :

$$m_i = \frac{1}{\sqrt{5}} \left[\left(\frac{3 + \sqrt{5}}{2} \right)^i - \left(\frac{3 - \sqrt{5}}{2} \right)^i \right] \approx 1.17 \cdot (2.618)^{i-1} \quad (33)$$

$$m_i = \begin{cases} 3 \cdot 2^{N-1} - 2^{N-i} - 2^{1+N/2} + 2 & \text{for } N = 2, 4, 6.. \\ 3 \cdot 2^{N-1} - 2^{N-i} - 3 \cdot 2^{(N-1)/2} + 2 & \text{for } N = 3, 5, 7.. \end{cases} \quad (34)$$

where N is the number of channels.

Series (33) is derived from the recursive expression (26) proposed by Sakai and Parry [6], expressed in closed form by Brooks *et al.* [8]. Series (34) is given by Blotejkaer *et al.* [11]. As an example, we show the two series for a twelve channel system :

Series (33)	1	3	8	21	55	144	377	987	2 584	6 765	17 711	46 368
Series (34)	3 970	4 994	5 506	5 762	5 890	5 954	5 986	6 002	6 010	6 014	6 016	6 018

We observe that series (34) has the smallest m_{12} , i.e., the smallest maximum optical delay. Hence series (34) is more compact and more advantageous in the sense that it allows shorter optical delays. However in series (33), the terms do not depend explicitly on the number of channels and, hence, for a system designed for a given channels, more channels can be added without changing the optical delays of the existing channels. In contrast, if another channel is to be added in a system designed using series (34), the system requires complete redesign. The starting value τ_1 is still determined using the curves of figure 9 which can be extended to series architectures. For instance, for a 12-channel system ruled by series (33) and powered by a Gaussian source with a coherence length $L_c = 30$ micrometers (e.g. a superluminescent diode), crosstalk of -25 dB requires a starting value of $\tau_1 = 45$ micrometers and a maximum optical delay of $\tau_{12} = 270\ 765$ micrometers. This shows clearly a practical limitation of the number of transmitters, that is a drawback in comparison with parallel topologies. Note however that series topologies are unique known configurations allowing signals to be multiplexed optically with a single source.

6. Applications.

6.1 INTEGRATED COHERENCE MODULATORS. — The previous sections show that coherence multiplexing can play an important role in the future networks for optical communications. However the construction of modulators matched to coherence modulation is the most serious problem at present. Bulk electro-optic modulators based on Pockels effects in birefringent materials have been proposed to demonstrate the parallel and series topologies and to verify the basic concepts in multimode and single mode fiber transmissions [10, 12, 13]. Integrated phase modulators inserted in one arm of fiber Mach-Zehnder interferometers having a large path-imbalance is a tentative solution usable for demonstration purposes only. The sensitivity of such devices to temperature or to mechanical vibrations is a major drawback. Integrated Mach-Zehnder type modulators could be used. However, their geometry is usually designed to introduce slight imbalanced paths ($< \lambda/4$), yielding optical delays much smaller than the coherence length of the source.

Hence, new integrated modulators have to be developed. An LiNbO_3 integrated Mach-Zehnder interferometer with a large path-imbalance between the arms has been proposed recently [14]. The device is shown in figure 10. The path-imbalance is created by a proton exchanged process located on one arm. Proton exchange between Li^+ ions from lithium niobate and H^+ protons from an acid source (e.g. melted benzoic acid in which one arm of the interferometer is immersed) occurs to yield a new propagation medium ($\text{H}_x\text{Li}_{1-x}\text{NbO}_3$) with an extraordinary refractive index higher than that of lithium niobate. Hence, the proton exchange process modifies the effective index of the guided mode. Path-differences of several

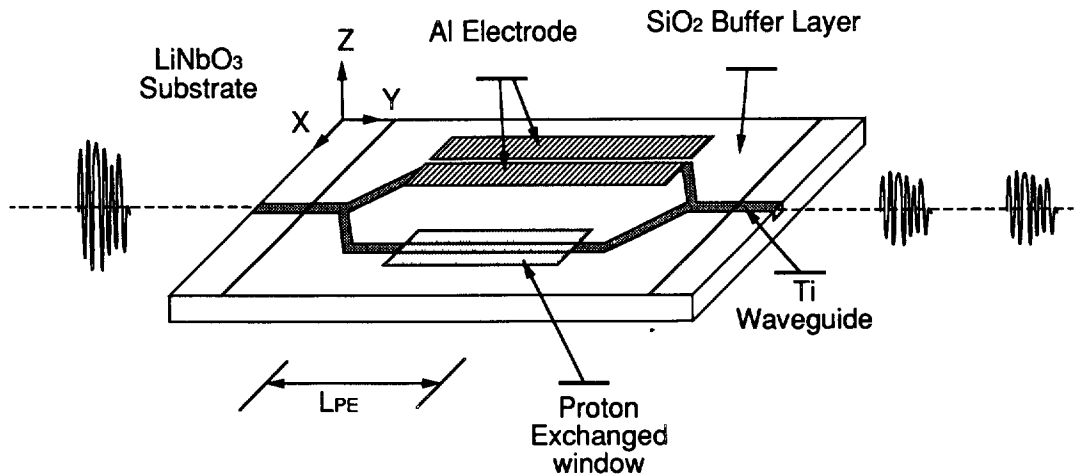


Fig. 10. — Coherence modulator integrated on a LiNbO_3 substrate.

hundreds of micrometers can be obtained. The electrodes on the other arm induce an electric field which, in turn, results in a modulation of the effective index of the guided wave by Pockels effect. Half-wave voltages of 15 V at 1 300 nm wavelength have been obtained. This device is probably the first integrated system showing that coherence modulation of light can be performed using integrated optics technology. This opens up new applications since it permits integration of several coherence modulators as well as several receiving interferometers to be carried out on a single chip. Bandwidths up to 6 GHz have just been demonstrated at our laboratory [26].

6.2 OPTICAL COMMUNICATIONS. — Electro-optic coherence modulators such as described above can be used to generate a sequence of optical delays larger than the coherence length with a potential bandwidth of several tens of GHz. Multiplexing experiments over several kilometer-long multimode and singlemode fibers have been conducted using multimode laser diodes and superluminescent diodes [12, 13, 15, 16]. Practically, the maximum number of channels in series topologies is estimated to be limited to about 10 by the propagation losses in the cascaded modulators (3 dB loss power per modulator) for -50 dBm detection threshold at the detectors and a data rate of 140 Mbit/s. Very recent results have also been obtained with integrated modulators which allow 30 km long transmissions on a singlemode fiber at 400 Mbit/s [17]. An unexpected application deals with two-way transmission on a single fiber [18, 19]. In that case, coherence modulation of light is used together with conventional intensity modulation to transmit data in two directions simultaneously through one fiber and with a single light source. A bit-error-rate smaller than 10^{-10} has been demonstrated. The peculiarity of this method is that it is probably the only optical method which allows bidirectional data transmissions with identical modulation rates in the two directions. Also note that other configurations combining both series and parallel topologies can be used to increase the number of channels. Of the several possible architectures, a parallel system topology in which a single source is used to coherence-multiplex several signals for telecommunications applications was recently reported by Blair and Cormack [20] who studied the influence of the source linewidth on the system multiplexing capacity. Recently, interest has been shown in applying coherence multiplexing principles to high speed (> 10 Gbit/s) interprocessor links in parallel computers using integrated optics technology [21].

6.3 ARRAY OF SENSORS. — Interest in sensing has also grown since Al-Chalabi *et al.* [22] and Brooks *et al.* [8] pointed out that the method also applies to multiplex sensor arrays using a single source.

The sensor arrays are formed by series of unbalanced fiber Mach-Zehnder interferometers powered by a laser diode with a short coherence length relative to the path-imbalance of the sensing interferometers. The fiber Mach-Zehnder interferometers used exhibit long branches (> 10 m) in order to obtain a high sensitivity, especially for hydrophone applications in which the signals to detect may be very weak. The use of a singlemode laser source with a relatively long coherence length (> 1 m) is advantageous in that case as it facilitates more straightforward matching between the fiber Mach-Zehnder interferometer pairs forming the sensor array. However, phase-induced intensity noise which is increasingly important with increasing the coherence length limits the sensitivity of the system and can severely reduce the dynamic range of the system. A method for the reduction of this excess phase noise was proposed by Kersey and Dandridge [7], using diode laser frequency modulation to effect a frequency translation of the excess noise power. They reported an improvement of 40 dB in minimum detectable phase shift sensitivity and demonstrated a sensor with a sensitivity down to $45 \mu\text{rad}/\sqrt{\text{Hz}}$. A sensor specially designed for subnanometric measurements is described in reference [23]. Considerations on noise performance in sensing are discussed in reference [9]. Recently, a coherence-multiplexed quasi-distributed sensor based on the retardation properties of birefringent fibers has also been proposed by Turpin *et al.*, and Guresmoli *et al.* [24].

6.4 SIGNAL PROCESSING AND OPTICAL COMPUTING. — Recent work has also been directed towards the implementation of an electro-optic systolic processor, using coherence modulation principles and performing in parallel fast-matrix vector products. This type of operations play an important role in a number of signal processing applications involving FFT, digital correlations and convolutions, such as pattern recognition or radar signal processing for instance. The processor is based on the series configuration. It consists of an array of cascaded electro-optic coherence modulators in tandem with decoding modules operating as receiving interferometers. In that case, the coherence modulators are used both to multiplex data on a light beam and to compute multiplications. A description of the system is given in reference [25] which also gives the principle of operation in the case of matrix-vector products. The computing speed of the demonstrator constructed at our laboratory is currently of 50 millions of operations per second and the size of the processed matrices is 5 lines, 10^4 columns.

7. Conclusion : is the term « coherence modulation » the most appropriate ?

The point of view developed in this paper is based on models in which light is considered as stochastic fields characterized by second-order moments, i.e. coherence functions. The reasons for which the term « coherence modulation » is used are mainly based on the fact that side lobes of coherence are generated when light propagates in a series of interferometers. This means clearly that the temporal coherence of light suffers a modulation. However the authors are often asked whether coherence modulation is the most appropriate term to describe the physical principles. Indeed another approach consists in considering the information carrier is formed physically by optical delays, rather than by the coherence degree itself. For instance, in the multiplexing schemes in figures 4 and 5, each channel corresponds to a given optical delay τ_i which behaves as an information carrier for the signal ; the latter is imprinted on light by modulating the carrier, i.e., the optical delay around the mean value τ_c . Hence the method can be termed « path-difference modulation », which is more appropriate since it gives a straightforward description of signal encoding.

An alternative point of view is also possible when noticing that an interferometer with a path-difference greater than the coherence length is equivalent to a spectral filter with a sinusoidal transmission curve. Then the series of interferometers of figure 4, as well as the receiving interferometer, can be considered as cascaded spectral filters in tandem with a receiving spectral filter whose transmission curve is tuned to select the desired channel. The method can thus be also named « spectral modulation », since many aspects are similar to the so-called wide spectrum transmission methods in signal processing. The term « coherence modulation », which rather denotes a statistical description, was first introduced by Brooks *et al.* [8] in the area of sensors, independently of previous works in the field of optical communications in which the previous considerations were used to describe the physical principles [4, 5], and is now widely used in the international optical community. All these terms are equivalent.

References

- [1] See for instance BORN M., WOLF E., Principles of Optics, 6th Edition (Pergamon Press), pp. 503-505.
- [2] See for instance BORN M., WOLF E., Principles of Optics, 6th Edition (Pergamon Press), pp. 364-367.
- [3] FLOURNOY P. A., MCCLURE R. W., WINTJES G., White light interferometric thickness gauge, *Appl. Opt.* **11** (1972) 1907-1915.
- [4] DELISLE C., CIELO P., Multiplexing in optical communications by interferometry with a large path-length difference in white light, *Canadian J. Phys.* **54** (1976) 2322-2331.
- [5] GOEDGEBUER J. P., SALCEDO J., VIÉNOT J. Ch., Multiplex communication via electro-optic phase modulation of white light, *Optica Acta* **29** (1982) 471-477.
- [6] SAKAI I., PARRY G., Multiplexing interferometric fibre sensors by frequency modulation techniques, Tech. Dig. Third Int. Conf. Optical Fiber Sensors (San Diego, Feb. 13-14, 1985) pp. 128-130.
- [7] KERSEY A. D., DANDRIDGE A., Phase-noise reduction in coherence-multiplexed interferometric fibre sensors, *Electron. Lett.* **22** (1986) 616-618.
- [8] BROOKS J. L., YOUNGQUIST R. C., WENTWORTH R. H., TUR M., KIM B. Y., SHAW H. J., Coherence multiplexing of fiber-optic interferometric sensors, *J. Lightwave Technol.* **3** (1985) 1062-1072.
- [9] WENTWORTH R. H., Theoretical noise performance of coherence-multiplexed interferometric sensors, *J. Lightwave Technol.* **7** (1989) 941-956.
- [10] GOEDGEBUER J. P., HAMEL A., PORTE H., Analysis of optical crosstalk in coherence multiplexed systems employing a short coherence laser diode with arbitrary power spectrum, *IEEE J. Quantum Electron.* **26** (1990) 1217-1226.
- [11] BLOTEKJAER K. J., WENTWORTH R. H., SHAW H. J., Choosing Relative Optical Path Delays in Series-Topology Interferometric Sensor Arrays, *J. Lightwave Technol.* **5** (1987) 229-235.
- [12] PORTE H., GOEDGEBUER J. P., HAMEL A., Two TV channel multimode fibre link using a single multimode laser diode and path-difference multiplexing, *Electron. Lett.* **22** (1986) 1189-1191.
- [13] GOEDGEBUER J. P., PORTE H., HAMEL A., Electro-optic Modulation of multilongitudinal mode laser diodes: demonstration at 850 nm with simultaneous data transmission by coherence multiplexing, *IEEE J. Quantum Electron.* **23** (1987) 1135-1144.
- [14] MOLLIER P., PORTE H., GOEDGEBUER J. P., Proton exchanged imbalanced Ti: LiNbO₃ Mach-Zehnder modulator, *Appl. Phys. Lett.* **60** (1992) 274-276.
- [15] GOEDGEBUER J. P., FERRIÈRE R., HAMEL A., Polarization-independent transmission on a single mode fiber using coherence modulation of light, *IEEE J. Quantum Electron.* **27** (1991) 1963-1967.

- [16] GOEDGEBUER J. P., HAMEL A., Coherence Multiplexing Using a Parallel Array of Electrooptic Modulators and Multimode Semiconductor Lasers, *IEEE J. Quantum Electron.* **23** (1987) 2224-2237.
- [17] HAMEL A., MATHIEU M. P., PORTE H., FERRIÈRE R., GOEDGEBUER J. P., Proc. EFOC/LAN 91 (London-June 91).
- [18] GOEDGEBUER J. P., HAMEL A., A novel modulation method for bidirectional transmissions on a single optical fiber, *Appl. Phys. Lett.* **57** (1990) 1384-1386.
- [19] GOEDGEBUER J. P., HAMEL A., PORTE H., Full bidirectional fiber transmission using coherence-modulated lightwaves, *IEEE J. Quantum Electron.* **28** (1992) 2685-2691.
- [20] BLAIR D. A., CORMACK G. D., Optimal source linewidth in a coherence multiplexed optical fiber communications system, *J. Lightwave Technol.* **10** (1992) 804-810.
- [21] CHU K. W., DICKEY F. M., Optical Coherence multiplexing for interprocessor communications, *Opt. Eng.* **30** (1991) 337-344.
- [22] AL-CHALABI S. A., CULSHAW B., DAVIES D. E. N., Proc. 1st International Conference on Optical Fiber Sensors (IEE) (1983) pp. 132-135.
- [23] FERDINAND P., PAULET M., PILLON R., Proc. OPTO 87, Paris, May (ESI Publications. Paris) pp. 294-299.
- [24] TURPIN M., BREVINGON M., ROSAS D., Proc. Congrès Mesucora, Paris, pp. 116-117 ;
GURESOLI V., VAVASSORI P., MARTINELLI M., OFS 89, Springer Proceedings in Physics **44** (Heidelberg : Springer-Verlag) pp. 513-518.
- [25] GOEDGEBUER J. P., PORTE H., FERRIÈRE R., Recent advances in electro-optic coherence multiplexing, *Int. J. Optoelectron.* **6** (1991) 339-356.
- [26] GUTTERIEZ C., Private communication, 1993.